Photoluminescence quenching in peapod-derived double-walled carbon nanotubes

Toshiya Okazaki,[1,*] Shunji Bandow,[2] Goshu Tamura,[2] Yoko Fujita,[2] Konstantin Iakoubovskii,[3] Said Kazaoui,[1,3] Nobutsugu Minami,[3] Takeshi Saito,[1] Kazu Suenaga,[1] and Sumio Iijima[1,2]

[1]*Research Center for Advanced Carbon Materials, National Institute of Advanced Industrial Science and Technology (AIST), Tsukuba 305-8565, Japan*

[2]*Department of Materials Science and Engineering, 21st century COE (Nanofactory), Meijo University, 1-501 Shiogamaguchi, Tenpaku-ku, Nagoya 468-8502, Japan*

[3]*Nanotechnology Research Institute, AIST, Tsukuba 305-8565, Japan*

(Received 22 July 2006; published 5 October 2006)

Photoluminescence (PL) behavior of peapod-derived double-walled carbon nanotubes (DWNTs)—the simplest form among multiwalled carbon nanotubes—is investigated. Even though the optical absorption and the resonant Raman spectra show the characteristic features of DWNTs, the PL signals originated from DWNTs are severely suppressed. This suppression is a consequence of an interlayer interaction between the inner and the outer tubes that efficiently quenches the PL signals of the DWNTs.

DOI: 10.1103/PhysRevB.74.153404 PACS number(s): 78.67.Ch, 73.22.−f, 78.30.Na

An important breakthrough in the carbon nanotube spectroscopy came in 2002 when photoluminescence (PL) signals were recorded from isolated single-walled carbon nanotubes (SWNTs) that were wrapped with sodium dodecyl sulfate (SDS).[1,2] Since then, two-dimensional PL excitation and emission mapping has been widely recognized as a powerful tool for the characterization of the unique electronic properties of the SWNTs associated with their low dimensionality, and for the analysis of the detailed tubule distribution of the bulk samples.[3] Although PL properties of SWNTs are well established, it is yet unclear whether PL can be obtained from MWNTs. In particular, one might expect that the inner core tube is protected from the environment and its intrinsic optical properties are preserved.

Double-walled carbon nanotubes (DWNTs) may answer to the above question because they have the simplest structure among multiwalled carbon nanotubes (MWNTs), which make it easier to interpret the experimental observations. Recently, PL signals have been detected from DWNTs synthesized by chemical vapor deposition (CVD) and attributed to the inner shells of DWNTs.[4] However, it should be noted that CVD-grown DWNT samples usually are mixed with small amounts of SWNTs that have similar diameters as the inner cores of the DWNTs. Therefore, it is uncertain whether the detected PL originated from the isolated SWNTs or truly from the inner shells of DWNTs. Alternatively, DWNTs can be synthesized by thermal treatment of SWNTs encapsulating C_{60} molecules (the so-called "peapods").[5] The peapod-derived DWNT samples also contain undesirable SWNTs, however there is a clear difference between the SWNTs existing in the CVD sample and those of peapod-derived DWNTs: The diameters of the residual SWNTs in the former samples are similar to those of the inner DWNT shells and in the latter samples to those of the outer shells. Consequently, the peapod-derived DWNTs are more suitable for studying PL from the inner tubes. Furthermore, comparative measurements between DWNTs and the pristine SWNTs are available for the peapod-derived samples. This allows us to investigate the PL behavior of the outer tubes after forming the inner tube structures.

Here we report a detailed study of PL from the peapod-derived DWNTs, together with optical absorption and resonant Raman spectroscopy. Our results reveal that the emission from both the inner tubes and the outer ones is effectively quenched due to their interlayer interaction.

The DWNTs studied here were synthesized by annealing of C_{60} peapods at 1200 °C.[5] The pristine SWNTs with diameter (d_t) ranging in ~1.2–1.4 nm were produced by the pulsed laser vaporization of an Fe-Ni–containing carbon target. Aqueous micellar solutions of DWNTs were prepared in a similar way to the procedure described by Bachilo *et al.*[2] Briefly, DWNTs (~0.5 mg) were dispersed in ~15 ml of D_2O containing 1 wt % of sodium dodecylbenzene sulfonate (SDBS) by sonication for 10 min using a 200 W homogenizer (Sonics VCX500).[6,7] The resultant solution was then centrifuged at 127 600 g for 1 h (Hitachi CP 100MX centrifuge) and the supernatant of the upper ~2/3 volume was collected. Transmission electron microscope (TEM) images were taken with a JEOL 2100F microscope operated at 120 kV. The TEM specimen was prepared by casting a few droplets of a DWNT-SDBS-D_2O solution onto a carbon microgrid. Optical absorption spectra were recorded with a Shimadzu UV-3150 spectrometer. Low-resolution resonant Raman spectra were measured with a single-grating monochromator equipped with an InGaAs diode array and an appropriate rejection filter, using a tunable Ti-sapphire laser (Spectra Physics 3900S) for excitation. High-resolution (1 cm^{-1}) Raman spectra were measured with a Bruker RFS100 Fourier-transform (FT) Raman spectrometer using 1064 nm laser excitation. PL mapping in a detection range of 950–1630 nm was carried out with a Horiba SPEX Fluorolog 3-2 Triax spectrometer equipped with a near-infrared photomultiplier (Hamamatsu H9170-75). PL mapping at a longer wavelength (1200–1800 nm) was performed with a home-built setup utilizing a tunable Ti-sapphire laser for excitation and a Jasco FTIR-800 spectrometer, equipped with an IR-enhanced InGaAs diode for detection.

Figure 1 shows the TEM images of SDBS-suspended DWNTs after centrifugation. It is confirmed that the nanotubes are largely and uniformly covered by the surfactant that appears with typical image contrast for amorphous materials. Although the isolated DWNTs were frequently observed, most of them formed bundles. We suspect that the

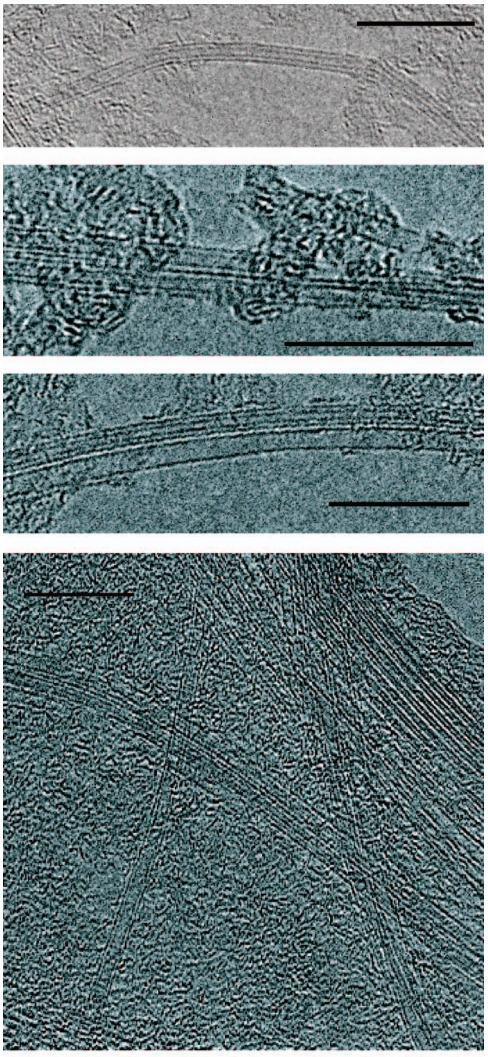

FIG. 1. (Color) HRTEM images of DWNT SDBS D_2O. Scale bar=10 nm.

bundling took place when the sample was dried on the TEM grid. The HRTEM images indicate that about one half of the nanotubes have the double-walled structure.

Figure 2(a) presents an UV-vis-NIR absorption spectrum of a DWNT-SDBS-D_2O solution, together with the reference spectrum of the pristine SWNT SDBS D_2O. Those spectra show characteristic peaks associated with the interband transitions. The broad features in the 800–1100 nm range belong to the second van Hove transitions (E_{22}^S) in semiconducting nanotubes with $d_t \sim 1.2-1.4$ nm. The peaks in the ranges 400–600 nm and 600–800 nm can be assigned to the third van Hove transitions (E_{33}^S) of the semiconducting nanotubes and E_{11}^M transitions in the metallic nanotubes, respectively. Besides those features, DWNTs show prominent peaks at ~1037 and ~598 nm (marked by arrows), which, based on their transition energies, can be attributed to the E_{11}^S and E_{22}^S transitions of the inner tubes, respectively. Note that the E_{11}^S transitions of the inner tubes ($d_t \sim 0.7$ nm) coincidently overlap with the E_{22}^S features of the outer tubes ($d_t \sim 1.4$ nm).

In order to investigate the origin of the absorption peak at

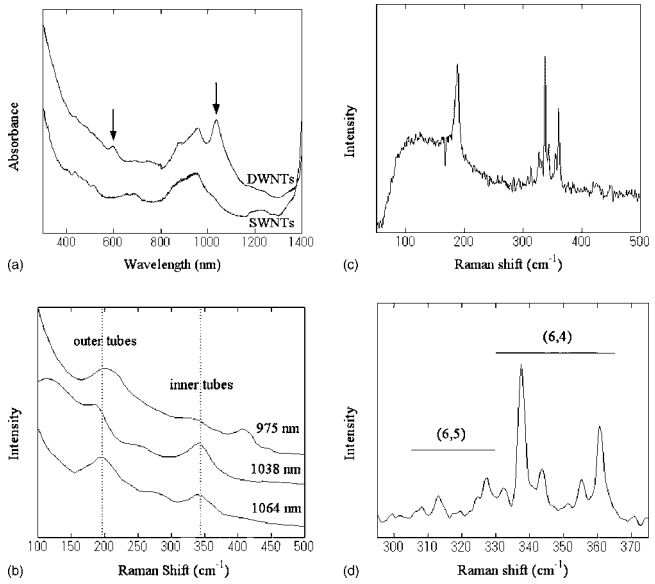

FIG. 2. (a) UV-vis-NIR absorption spectra of DWNT-SDBS-D_2O and SWNT-SDBS-D_2O solutions. (b) Low-resolution resonant Raman spectra of a DWNT-SDBS-D_2O solution excited at 975, 1038, and 1064 nm. (c) High-resolution resonant Raman spectrum of a DWNT-SDBS-D_2O solution excited at 1064 nm. (d) An expanded view of the high-resolution Raman spectrum of the inner tubes.

~1037 nm, resonant Raman spectra were recorded using different excitation wavelengths. The top spectrum of Fig. 2(b) was recorded under 975 nm excitation, which should resonantly excite the E_{22}^S transitions of either outer tubes of DWNTs or SWNTs [see Fig. 2(a)]. Indeed, the radial breathing mode (RBM) of vibration of the outer DWNT shells (or of the residual SWNTs) is clearly observed at ~200 cm^{-1}, which corresponds to $d_t \sim 1.3$ nm. Another RBM appears at ~345 cm^{-1} when the excitation wavelength (1038 nm) is resonant with the E_{11}^S absorption of the inner tubes. The peak intensity decreased at the slightly longer excitation wavelength of 1064 nm, whereas the RBM of the outer tubes relatively increased. This behavior matches the wavelength dependence of the absorption spectrum of the DWNTs [Fig. 2(a)], especially of the 1037 nm peak associated with the inner tubes, thus suggesting a similar origin to the 1037 nm absorption peak and the 345 cm^{-1} RBM.

Figure 2(c) shows a high-resolution Raman spectrum of a DWNT-SDBS-D_2O solution measured at 1064 nm excitation. A set of strong and narrow lines observed in the spectral range from 310 to 370 cm^{-1} is a characteristic feature of the inner tubes of peapod-derived DWNTs.[8] Those peaks have been recently assigned to the (6,4) and (6,5) tubes.[9] Strong (6,4) components indicate that substantial amounts of (6,4) tubes belong to the inner shells of our DWNTs. Note that the E_{11}^S and E_{22}^S transition wavelengths of the (6,4) SWNT were estimated at 873 and 578 nm, respectively, in the SDS micellar solution.[10] These wavelengths are shorter than those observed in Fig. 2(a) (~1037 and ~598 nm). The redshifts observed in the present experiment are consistent with the theoretical predictions[11,12] and could be attributed to the interaction between the inner and outer tubes as well as the PL quenching, as discussed below.

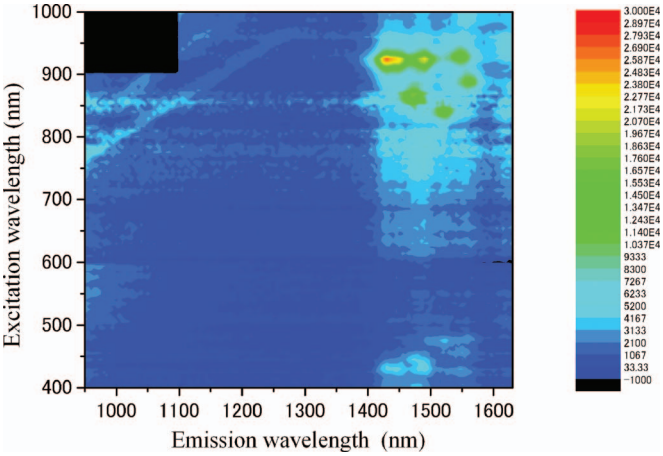

FIG. 3. (Color) Two-dimensional (2D) photoluminescence contour map of a DWNT-SDBS-D_2O solution.

If the inner tubes were luminescent, then the PL associating with the E_{11}^S transitions could be observed (at least) at ~1037 nm by the E_{22}^S excitation at ~598 nm. However, despite the high concentration of DWNTs, no PL could be detected under 598 nm excitation (see Fig. 3). This implies that PL from the inner tubes is severely quenched, possibly due to the presence of the outer tubes. On the other hand, strong PL peaks are observed in the excitation range of 800–950 nm and the detection range of 1400–1600 nm. Those peaks can be unambiguously assigned to the E_{11}^S emission from the semiconducting tubes with $d_t \sim 1.2–1.4$ nm due to photoexcitation of E_{22}^S transitions. One could expect that the excitation of the inner tubes would be transferred to the outer DWNTs resulting in additional PL from those outer tubes. In this case, extra PL signals should be observed at ~598 nm excitation. However, no such signals could be detected (see Fig. 3).

The absence of PL from the outer tubes under the photoexcitation of E_{22}^S transitions of the inner tubes implies that the efficient and nonradiative relaxation paths exist between the van Hove states of E_{11} for the outer tubes. We then performed a detailed comparison of PL from the outer shells of the DWNTs and from the pristine SWNTs to check such a relaxation path. Figure 4(a) shows a 2D PL contour map of a DWNT-SDBS-D_2O solution measured in the longer wavelength region. The map reveals an apparent decrease in PL signals from the outer tubes with a larger diameter [e.g., (12,7) and (10,9) tubes] as compared to the corresponding signals from the pristine SWNTs [Fig. 4(b)]. In order to distinguish the difference between the DWNTs and SWNTs of the PL intensities, we plotted the PL intensity ratio of DWNTs and the corresponding pristine SWNTs (I_{PL}^{DW}/I_{PL}^{SW}) as a function of the tube diameter d_t [Fig. 4(c)] Even though PL peak features for the DWNTs and SWNTs are quite similar [Figs. 4(a) and 4(b)], the values of I_{PL}^{DW}/I_{PL}^{SW} decrease stepwise at $d_t \sim 1.27$ nm, as indicated by the dotted line in Fig. 4(c). It is worth noticing that theoretical calculations predict that $d_t \sim 1.28$ nm is the smallest limit of the tube diameter for encasing the C_{60} molecules,[13] which is surprisingly close to the threshold value for the PL reduction deduced in Fig. 4(c). This agreement may suggest that the formation of the inner

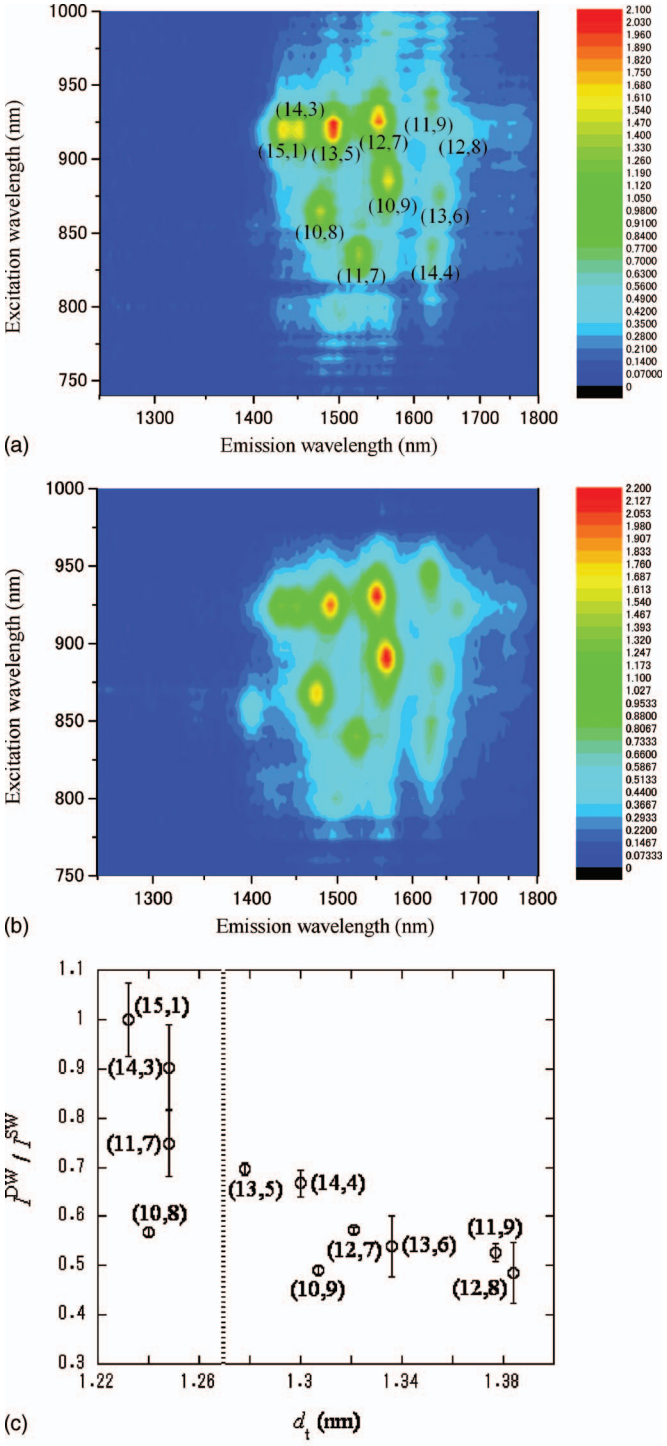

FIG. 4. (Color) 2D PL contour maps of (a) DWNT-SDBS-D_2O and (b) SWNT-SDBS-D_2O solutions in the longer wavelength region. (c) PL intensity ratio between DWNTs and SWNTs (I^{DW}/I^{SW}) as a function of a tube diameter, where each PL intensity ratio was normalized to that of a (15,1) tube.

shells in the peapod-derived DWNTs results in the quenching of PL by the outer DWNTs.

Simple geometrical consideration of the structural transformation from peapod to DWNT suggests the length of the inner tube to be ~2/3 of the outer tube and its remaining

space is empty even if the filling yield of C_{60} is 100%.[5] Assuming that DWNT formation results in the strong (>10 times) quenching of PL from the outer tubes, we might, expect a ~70% reduction of PL from the DWNTs with $d_t > 1.27$ nm. However, our PL measurements indicate a decrease of ~30–60 % [Fig. 4(c)].[14] This somewhat low-PL quenching efficiency might suggest that the filling yield of C_{60} is not 100%, but ~70%. Considering that the present DWNT sample contains the residual SWNTs having $d_t < 1.27$ nm and thus are incapable of encapsulating C_{60} molecules, this estimate is consistent with our TEM observations of the C_{60} peapods (~60%).

The intertube interaction may cause a downshift of the energy levels and even closure of the band gap. Such hybridization of the electronic structures of the inner and outer tubes has been argued theoretically.[11,12] For example, the π^* states of the inner (7,0) tube overlap with those of the outer $(n,0)$ tubes (n=16, 17, 19, and 20), which causes the metallization of the resulting DWNTs.[11]

Recently, a 1D metallic character for the inner tubes of peapod-derived DWNTs has been deduced from ^{13}C-NMR studies.[15] Charge transfer between the inner and outer DWNT shells was suggested as one of the possible reasons for this metallic behavior. However, in case of such a charge transfer, absorption and Raman signals from one of the shells should be significantly reduced. This is not observed in our spectra, thus rendering the charge transfer unlikely.

Another important prediction from the theory is that the interaction between the inner and outer shells in the DWNT strongly depends on the interlayer distance[11,12]—naturally, the larger the distance, the weaker the interaction. This tendency might explain the previous observation of PL from CVD DWNTs.[4] In the peapod-annealing technique, the inner tubes are created secondarily by annealing the existing SWNTs, while the inner and outer shells are simultaneously grown in the CVD process. A recent resonant Raman study suggests that the annealing first creates inner tubes with relatively narrow diameters, and then these diameters gradually increase during annealing, thereby decreasing the interlayer distance.[8] In the present case, the diameter of the outer tubes was estimated to be 1.278–1.384 nm from the PL map (Fig. 4). The diameters of the possible inner (6,4) and (6,5) tubes are 0.692 and 0.757 nm, respectively.[2] This indicates that the interlayer distance is less than ~0.346 nm. On the other hand, CVD-DWNTs in Ref. 4 have a much broader diameter distribution. The diameters were estimated to be 0.5–2.5 and 1.3–3.3 nm for the inner and the outer tubes, respectively. A broader diameter distribution might result in the broader distribution of the interlayer spacing. It is therefore likely that the CVD sample contains a significant fraction of DWNTs with the larger interlayer distance (much more than 0.346 nm)[16] and they can show PL signals.

It has been established that the PL behaviors of SWNTs are dominated by the Coulomb interaction between the optically produced electron-hole pairs (exitons).[17] The exciton binding energy was estimated to be ~0.420 eV for 0.8 nm SWNTs. If the exciton effects are affected by forming a double-wall structure, the binding energy is expected to decrease due to the lack of the low dimensionality. Assuming that the outer tubes observed here (Fig. 4) have the binding energy of ~0.420 eV,[18] the band-gap energies of the first and second van Hove singularities become ~1.3 and ~1.8 eV, respectively, which corresponds to the emission and excitation wavelengths of ~1000 and ~700 nm, respectively. Since the exciton effect might be smaller for DWNTs, PL peaks should be shifted to the shorter wavelength ranges 1000–1400 nm for emission and 700–800 nm for excitation after forming a double-wall structure. However, any additional PL peak was not observed in the corresponding region (Fig. 3). It is thus unlikely that the exciton effects on DWNTs are responsible for the PL quenching observed here.

In summary, the experimental results suggest that the electronic properties of DWNTs are rather complex and strongly depend on their structures and synthesis conditions. The interlayer distance might be an important parameter that governs the optical properties of DWNTs. A decrease in the interlayer distance enhances the interaction between the inner and outer shells, resulting in the efficient PL quenching. Based on these results, one might anticipate low PL efficiencies for MWNTs. Indeed, the interlayer distance in MWNTs is significantly smaller than in the DWNTs,[19] thus resulting in strong PL quenching.

We thank H. Kataura (AIST), S. Okada (Tsukuba University), and T. Nakanishi (AIST) for fruitful discussions.

*Author to whom correspondence should be addressed; Email address: toshi.okazaki@aist.go.jp

[1] M. J. O'Connell *et al.*, Science **297**, 593 (2002).
[2] S. M. Bachilo *et al.*, Science **298**, 2361 (2002).
[3] R. B. Weisman, in *Applied Physics of Carbon Nanotubes: Fundamentals of Theory, Optics and Transport Devices*, edited by S. V. Rotkin and S. Subramoney (Springer, Berlin, 2005), pp. 183–202.
[4] T. Hertel *et al.*, Nano Lett. **5**, 511 (2005).
[5] S. Bandow *et al.*, Chem. Phys. Lett. **337**, 48 (2001).
[6] T. Okazaki *et al.*, Nano Lett. **5**, 2618 (2005).
[7] T. Okazaki *et al.*, Chem. Phys. Lett. **420**, 286 (2006).
[8] S. Bandow *et al.*, Chem. Phys. Lett. **384**, 320 (2004).
[9] R. Pfeiffer *et al.*, Phys. Rev. B **72**, 161404 (2005).
[10] R. B. Weisman and S. M. Bachilo, Nano Lett. **3**, 1235 (2003).
[11] S. Okada and A. Oshiyama, Phys. Rev. Lett. **91**, 216801 (2003).
[12] W. Song *et al.*, Chem. Phys. Lett. **414**, 429 (2005).
[13] S. Okada *et al.*, Phys. Rev. Lett. **86**, 3835 (2001).
[14] Note that a comparison of absolute PL intensities between the different samples includes several uncertain factors, such as concentration. Here we assume that the PL intensities of (15,1) tubes are the same in the DWNT and SWNT samples, i.e., that $I_{PL}^{DW}/I_{PL}^{SW}=1$, because the (15,1) tube is too narrow to encapsulate C_{60} molecules (see text).
[15] P. M. Singer *et al.*, Phys. Rev. Lett. **95**, 236403 (2005).
[16] W. Ren *et al.*, Chem. Phys. Lett. **359**, 196 (2002).
[17] F. Wang *et al.*, Science **308**, 838 (2005).
[18] The binding energy of ~0.420 eV is considered to be the upper limit for the outer tubes (d_t=1.278–1.384 nm) because it decreases as the tube diameter increases [see T. Ando, J. Phys. Soc. Jpn. **74**, 77 (2005)].
[19] T. Hiraoka *et al.*, Chem. Phys. Lett. **382**, 679 (2003).